

# Topological Gluon Mass and Shear Viscosity of the Quark–Gluon Plasma

Debmalya Mukhopadhyay  
Independent Researcher  
Howrah, India  
debphys.qft@gmail.com

## Abstract

The quark–gluon plasma produced in relativistic heavy–ion collisions behaves as a nearly perfect fluid characterized by an exceptionally small shear viscosity to entropy density ratio. Understanding the microscopic origin of this small viscosity remains an important problem in the theory of strongly interacting matter. In this work we investigate the transport properties of a gluonic plasma in a non–Abelian gauge theory in which gluons acquire a gauge–invariant mass through a topological  $B \wedge F$  interaction. Integrating out the antisymmetric tensor field generates an effective massive gluon propagator that modifies the infrared behaviour of gluon exchange processes. Using relativistic kinetic theory and the Boltzmann transport equation we compute the shear viscosity of the plasma and derive the corresponding transport cross section for gluon scattering. The presence of the topological gluon mass provides a natural infrared regulator for  $t$ –channel gluon exchange, removing the divergence that appears in perturbative QCD with massless gluons. We show that when the topological mass scale is comparable to the soft momentum scale of the plasma,  $m \sim gT$ , the resulting viscosity to entropy density ratio naturally falls in the range inferred from hydrodynamic analyses of heavy–ion collision experiments. These results suggest that topological mass generation may provide a simple microscopic mechanism contributing to the near–perfect fluidity of the quark–gluon plasma.

**Keywords:** Quark–gluon plasma, transport coefficients, topological mass generation, relativistic kinetic theory.

**PACS numbers:** 12.38.Mh, 11.15.-q, 24.85.+p, 52.27.Ny, 25.75.-q.

# 1 Introduction

Quantum chromodynamics (QCD) predicts that strongly interacting matter under extreme conditions of temperature and density undergoes a phase transition from a hadronic phase to a deconfined state of quarks and gluons known as the quark–gluon plasma (QGP) [1, 2, 3]. Such a state of matter is believed to have existed in the early universe and can be recreated experimentally in relativistic heavy–ion collisions at facilities such as the Relativistic Heavy Ion Collider (RHIC) and the Large Hadron Collider (LHC).

One of the most remarkable properties of the QGP observed in heavy–ion collisions is its strong collective hydrodynamic behaviour. Experimental measurements of elliptic flow and other anisotropic flow coefficients indicate that the plasma behaves as an almost perfect fluid with extremely small viscosity [4, 5]. Hydrodynamic simulations of heavy–ion collisions suggest that the ratio of shear viscosity to entropy density lies in the range

$$0.08 \leq \frac{\eta}{s} \leq 0.20, \quad (1)$$

which is remarkably close to the lower bound

$$\frac{\eta}{s} = \frac{1}{4\pi}, \quad (2)$$

derived for a large class of strongly coupled gauge theories with gravity duals [6, 7]. The proximity of the QGP viscosity to this bound has generated considerable interest in understanding the microscopic origin of this strongly coupled behaviour.

In the weak coupling regime the shear viscosity of a gluonic plasma can be calculated using relativistic kinetic theory and the Boltzmann transport equation [8, 9, 10, 11]. Such perturbative calculations predict that the viscosity increases rapidly as the gauge coupling becomes small, leading to values of  $\eta/s$  that are typically much larger than those inferred from experimental data. Understanding the origin of the small viscosity observed in the QGP therefore remains an important theoretical problem.

A major difficulty in perturbative calculations of transport coefficients in QCD arises from the infrared behaviour of gluon exchange processes. The dominant contribution to gluon scattering at high temperature comes from  $t$ –channel exchange of nearly massless gluons. This leads to infrared divergences in the scattering cross section, which must be regulated by medium effects such as Debye screening [12, 13]. In thermal Yang–Mills theory the

infrared behaviour of gluon exchange is typically treated using Hard Thermal Loop (HTL) resummation [14, 12], which incorporates medium-induced screening effects into the gluon propagator.

In the framework considered in the present work such resummation is not required. Instead, the infrared behaviour of the gauge theory is regulated by a topological mechanism that generates a gauge-invariant mass for the gluon field. Specifically, the theory contains a topological  $B \wedge F$  interaction that couples the Yang-Mills field strength to an antisymmetric tensor field. Integrating out the tensor field generates an effective mass term for the gluon field while preserving gauge invariance. The resulting gluon propagator is modified according to

$$\frac{1}{k^2} \rightarrow \frac{1}{k^2 - m^2}, \quad (3)$$

so that the mass parameter  $m$  provides a natural infrared cutoff for gluon exchange processes.

Topologically massive gauge theories in four dimensions have been studied extensively in the context of gauge invariant mass generation [15, 16, 17, 18]. In these theories the gauge boson mass arises from a topological coupling between a one-form gauge field and a two-form tensor field, rather than from spontaneous symmetry breaking. This mechanism provides a natural infrared scale that can modify the dynamics of the gauge theory. Such topological mass generation mechanisms are also closely related to the appearance of a mass gap in the infrared sector of non-Abelian gauge theories. The existence of an infrared mass scale for gluonic excitations has long been expected to play an important role in the nonperturbative dynamics of QCD, including confinement and the structure of the strongly interacting vacuum.

The presence of a gluon mass changes the behaviour of scattering amplitudes at small momentum transfer and therefore alters the transport properties of the plasma.

In relativistic heavy-ion collisions the collective flow observables measured at RHIC and the LHC are particularly sensitive to the shear viscosity of the medium. Since the shear viscosity is controlled by the microscopic scattering rate of quasiparticles in the plasma, any mechanism that modifies the infrared behaviour of gluon exchange processes can have a direct impact on the hydrodynamic properties of the quark-gluon plasma. In particular, the topological mass regulates the infrared behaviour of the  $t$ -channel gluon propagator and leads to a finite transport cross section for gluon scattering.

Transport coefficients of the quark–gluon plasma, including shear viscosity and other dissipative properties, have been extensively studied using both perturbative and nonperturbative approaches [19, 20, 21].

The purpose of the present work is to investigate whether topological mass generation for gluons can provide a microscopic mechanism for the small viscosity observed in the quark–gluon plasma. Using kinetic theory we compute the shear viscosity of the plasma and determine how the modified gluon propagator affects the scattering rate of gluons in the medium. We further evaluate the ratio  $\eta/s$  and examine whether the presence of a topological gluon mass can naturally lead to values compatible with those inferred from heavy–ion collision experiments.

The paper is organized as follows. In Sec. 2 we review the topologically massive gauge theory and derive the propagator of the massive gluon field. In Sec. 3 we compute the gluon scattering amplitude and determine the transport cross section in the presence of the topological mass. In Sec. 4 we evaluate the shear viscosity using relativistic kinetic theory. In Sec. 5 we compute the ratio  $\eta/s$  and discuss the implications for the phenomenology of the quark–gluon plasma. Finally, Sec. 6 contains a summary and outlook.

## 2 Effective massive gluon propagator

In this section we derive the propagator of the gluon field that arises after integrating out the antisymmetric tensor field  $B_{\mu\nu}$ . This procedure generates an effective gauge–invariant mass for the gluon field.

### 2.1 Quadratic part of the action

To determine the propagators it is sufficient to consider the quadratic part of the Lagrangian density[22]

$$\mathcal{L} = -\frac{1}{4}F_{\mu\nu}F^{\mu\nu} + \frac{1}{12}H_{\mu\nu\lambda}H^{\mu\nu\lambda} + \frac{m}{4}\epsilon^{\mu\nu\rho\lambda}B_{\mu\nu}F_{\rho\lambda}. \quad (4)$$

For simplicity the non–Abelian color indices are suppressed in the Lagrangian density. The gauge fields should be understood as  $A_\mu = A_\mu^a T^a$  and  $B_{\mu\nu} = B_{\mu\nu}^a T^a$ , where  $T^a$  are the generators of the  $SU(N_c)$  gauge group. Repeated color indices are implicitly summed. The Yang–Mills field strength is

$$F_{\mu\nu}^a = \partial_\mu A_\nu^a - \partial_\nu A_\mu^a + g f^{abc} A_\mu^b A_\nu^c. \quad (5)$$

The field strength of the antisymmetric tensor field is

$$H_{\mu\nu\lambda}^a = (D_{[\mu} B_{\nu\lambda]})^a + gf^{abc} F_{[\mu\nu}^b C_{\lambda]}^c \quad (6)$$

where the fields  $A_\mu^a$ ,  $B_{\mu\nu}^a$  and  $C_\mu^a$  are in the adjoint representation of the  $SU(N_c)$  gauge group. To invert the kinetic operators we introduce gauge fixing terms

$$\mathcal{L}_{gf} = -\frac{1}{2\xi}(\partial_\mu A^\mu)^2 + \frac{1}{2\eta}(\partial_\mu B^{\mu\nu})^2. \quad (7)$$

The quadratic action can then be written in momentum space.

## 2.2 Momentum space representation

After Fourier transformation

$$A_\mu(x) = \int \frac{d^4k}{(2\pi)^4} e^{-ikx} A_\mu(k), \quad (8)$$

and similarly for  $B_{\mu\nu}$ . The quadratic Lagrangian becomes

$$\mathcal{L} = \frac{1}{2} A_\mu(-k) K^{\mu\nu}(k) A_\nu(k) + \frac{1}{4} B_{\mu\nu}(-k) M^{\mu\nu,\rho\sigma}(k) B_{\rho\sigma}(k) + \frac{im}{2} \epsilon^{\mu\nu\rho\lambda} B_{\mu\nu}(-k) k_\rho A_\lambda(k), \quad (9)$$

where

$$K^{\mu\nu}(k) = k^2 \eta^{\mu\nu} - k^\mu k^\nu. \quad (10)$$

The tensor kinetic operator is

$$M^{\mu\nu,\rho\sigma}(k) = k^2(\eta^{\mu\rho}\eta^{\nu\sigma} - \eta^{\mu\sigma}\eta^{\nu\rho}) + \eta^{\mu\rho}k^\nu k^\sigma - \eta^{\mu\sigma}k^\nu k^\rho - \eta^{\nu\rho}k^\mu k^\sigma + \eta^{\nu\sigma}k^\mu k^\rho. \quad (11)$$

## 2.3 Integrating out the tensor field

The partition function is

$$Z = \int \mathcal{D}A \mathcal{D}B e^{iS[A,B]}. \quad (12)$$

Since the action is quadratic in  $B_{\mu\nu}$  we can integrate it out exactly. The equation of motion for  $B_{\mu\nu}$  is

$$M^{\mu\nu,\rho\sigma} B_{\rho\sigma} + im\epsilon^{\mu\nu\rho\lambda} k_\rho A_\lambda = 0. \quad (13)$$

Solving for  $B_{\mu\nu}$  gives

$$B_{\mu\nu} = -\frac{im}{k^2} \epsilon_{\mu\nu\rho\lambda} k^\rho A^\lambda. \quad (14)$$

Substituting this solution back into the action produces an effective action depending only on  $A_\mu$ .

## 2.4 Effective action

The resulting effective quadratic Lagrangian becomes

$$\mathcal{L}_{eff} = -\frac{1}{4} F_{\mu\nu} F^{\mu\nu} + m^2 A_\mu \left( \eta^{\mu\nu} - \frac{k^\mu k^\nu}{k^2} \right) A_\nu. \quad (15)$$

This term represents a gauge invariant mass term for the gluon. The mass term obtained after integrating out the tensor field is transverse and therefore preserves gauge invariance. Unlike the Proca mass term  $m^2 A_\mu A^\mu$ , the operator

$$A_\mu \left( \eta^{\mu\nu} - \frac{\partial^\mu \partial^\nu}{\square} \right) A_\nu$$

projects onto the transverse component of the gauge field. As a result the gauge symmetry of the original theory remains intact.

## 2.5 Massive gluon propagator

The inverse propagator of the gluon field therefore takes the form

$$D_{\mu\nu}^{-1}(k) = (k^2 - m^2) \eta_{\mu\nu} - k_\mu k_\nu. \quad (16)$$

Inverting this tensor yields the propagator

$$D_{\mu\nu}(k) = \frac{-i}{k^2 - m^2} \left( \eta_{\mu\nu} - \frac{k_\mu k_\nu}{k^2} \right) - i\xi \frac{k_\mu k_\nu}{k^4}. \quad (17)$$

This propagator describes a massive vector boson with mass  $m$  while preserving gauge invariance. The topological  $B \wedge F$  interaction generates additional interaction vertices involving the tensor field  $B_{\mu\nu}$  and the gauge field. However, since the action is quadratic in  $B_{\mu\nu}$ , the tensor field can be integrated out exactly. The resulting effective theory contains a massive

gluon propagator while the explicit  $B_{\mu\nu}$  degrees of freedom no longer appear. Consequently the tree-level gluon scattering diagrams are the same as in Yang–Mills theory, but with the propagator modified to

$$\frac{1}{k^2 - m^2}. \quad (18)$$

The presence of this mass modifies the infrared behaviour of gluon exchange processes and will play a crucial role in determining the transport properties of the plasma. The propagator describes a massive vector excitation with three physical polarization states. In covariant gauges the propagator contains a gauge-dependent longitudinal component, while the physical propagating modes correspond to the transverse polarizations. A massive vector boson possesses three physical polarization states corresponding to two transverse modes and one longitudinal mode. However, in the high-temperature regime relevant for the quark–gluon plasma the dominant contribution to the transport cross section arises from the transverse gluon polarizations. The longitudinal contribution is suppressed by powers of  $m/E$  and will therefore be neglected in the present analysis. This approximation is justified in the high-temperature regime  $T \gg m$  where the dominant contribution to the transport cross section arises from transverse gluon polarizations. Topologically massive gauge theories in four dimensions have been studied extensively in the context of gauge invariant mass generation [15, 16, 17, 18, 22].

### 3 Gluon scattering and transport cross section

The scattering amplitudes are computed using the standard Feynman rules of Yang–Mills theory [23, 24]. In this section we calculate the gluon scattering amplitude in the presence of the topological gluon mass derived in the previous section. The resulting scattering cross section will determine the relaxation time and ultimately the shear viscosity of the plasma.

#### 3.1 Kinematics of gluon scattering

The dominant scattering process in a gluonic plasma is elastic two-body scattering

$$g(p_1) + g(p_2) \rightarrow g(p_3) + g(p_4). \quad (19)$$

The Mandelstam variables are defined as

$$s = (p_1 + p_2)^2, \quad (20)$$

$$t = (p_1 - p_3)^2, \quad (21)$$

$$u = (p_1 - p_4)^2. \quad (22)$$

These variables satisfy

$$s + t + u = 4m^2 \quad (23)$$

Since the gluons acquire a mass  $m$  through the topological mechanism discussed in Sec. II, the Mandelstam variables satisfy  $s + t + u = 4m^2$  rather than the massless relation  $s + t + u = 0$ .

### 3.2 Dominant scattering channel

The leading contribution to gluon scattering at high temperature arises from  $t$ -channel gluon exchange. Using the massive propagator derived previously

$$D_{\mu\nu}(k) = \frac{-i}{k^2 - m^2} \left( g_{\mu\nu} - \frac{k_\mu k_\nu}{k^2} \right), \quad (24)$$

the propagator in the  $t$  channel becomes

$$\frac{1}{t - m^2}. \quad (25)$$

The corresponding matrix element can be written as

$$\mathcal{M}_t = g^2 f^{abe} f^{cde} \frac{1}{t - m^2} \epsilon_1^\mu \epsilon_2^\nu \epsilon_3^\rho \epsilon_4^\sigma N_{\mu\nu\rho\sigma}, \quad (26)$$

where  $N_{\mu\nu\rho\sigma}$  represents the tensor structure arising from the triple-gluon vertices,

$$N_{\mu\nu\rho\sigma} = \Gamma_{\mu\nu\alpha}(p_1, p_2, -k) \left( g^{\alpha\beta} - \frac{k^\alpha k^\beta}{k^2} \right) \Gamma_{\rho\sigma\beta}(-p_3, -p_4, k), \quad (27)$$

with the triple-gluon vertex tensor

$$\Gamma_{\mu\nu\alpha}(p, q, r) = g_{\mu\nu}(p - q)_\alpha + g_{\nu\alpha}(q - r)_\mu + g_{\alpha\mu}(r - p)_\nu. \quad (28)$$

The full tree-level gluon scattering amplitude contains contributions from  $s$ -,  $t$ -, and  $u$ -channel exchange diagrams together with the four-gluon interaction vertex. In a high-temperature plasma the dominant contribution to momentum transport arises from small-angle scattering where the momentum transfer  $|t|$  is much smaller than  $s$ . In this kinematic regime the

$t$ -channel propagator is strongly enhanced, while the  $s$ - and  $u$ -channel contributions remain suppressed. For this reason we retain only the  $t$ -channel contribution in the calculation of the transport cross section.

The dominance of the  $t$ -channel contribution can be understood parametrically. In the small-angle scattering regime relevant for transport processes the momentum transfer satisfies  $|t| \ll s$ . The propagators appearing in the different channels scale as

$$\frac{1}{t - m^2}, \quad \frac{1}{s - m^2}, \quad \frac{1}{u - m^2}. \quad (29)$$

Since the typical center-of-mass energy in the plasma is  $s \sim T^2$  while the momentum transfer is of order  $|t| \sim g^2 T^2$ , the ratio of propagators behaves as

$$\frac{s}{|t|} \sim \frac{1}{g^2}. \quad (30)$$

For weak or moderately strong coupling this enhancement makes the  $t$ -channel exchange the dominant contribution to the scattering amplitude.

After averaging over initial colors and polarizations the squared matrix element becomes

$$|\mathcal{M}|^2 = \frac{9}{2} g^4 \frac{s^2 + u^2}{(t - m^2)^2}. \quad (31)$$

Because the gluons acquire a topological mass, the vector field in principle possesses three physical polarization states.

The completeness relation for a massive vector boson is

$$\sum_{\lambda} \epsilon_{\mu}^{(\lambda)}(p) \epsilon_{\nu}^{(\lambda)*}(p) = - \left( g_{\mu\nu} - \frac{p_{\mu} p_{\nu}}{m^2} \right). \quad (32)$$

However, in the high-temperature regime relevant for the quark-gluon plasma the typical gluon energy satisfies  $E \sim T$ , while the mass scale is assumed to be  $m \sim gT$ . The contribution of the longitudinal polarization to the scattering amplitude is therefore suppressed by powers of  $m^2/E^2 \sim g^2$ . To leading order in the weak-coupling expansion the dominant contribution to the transport cross section arises from transverse gluon polarizations, and the longitudinal contribution can be neglected.

### 3.3 Differential cross section

The differential cross section for two-body scattering is

$$\frac{d\sigma}{dt} = \frac{|\mathcal{M}|^2}{16\pi s^2}. \quad (33)$$

Substituting the matrix element gives

$$\frac{d\sigma}{dt} = \frac{9g^4}{32\pi} \frac{s^2 + u^2}{s^2(t - m^2)^2}. \quad (34)$$

Using the Mandelstam relation for massive gluons

$$s + t + u = 4m^2, \quad (35)$$

the variable  $u$  can be written as

$$u = 4m^2 - s - t. \quad (36)$$

In the kinematic regime relevant for a high-temperature plasma the typical center-of-mass energy satisfies  $s \gg m^2$  and  $s \gg |t|$ . In this limit the mass corrections to the Mandelstam variables are negligible and one may approximate

$$u \approx -s. \quad (37)$$

Consequently

$$s^2 + u^2 \approx 2s^2. \quad (38)$$

The detailed evaluation of the transport cross section is presented in Appendix A and B. The result can be written as

$$\sigma_{\text{tr}} = \frac{9g^4}{32\pi p^2} \ln\left(\frac{s + m^2}{m^2}\right). \quad (39)$$

In a thermal plasma the typical center-of-mass energy satisfies  $s \sim T^2$ . The transport cross section therefore becomes

$$\sigma_{\text{tr}} \approx \frac{9g^4}{32\pi T^2} \ln\left(\frac{T^2}{m^2}\right). \quad (40)$$

### 3.4 Physical interpretation

In perturbative QCD with massless gluons the transport cross section contains an infrared divergence arising from the  $t$ -channel exchange of nearly massless gluons. The differential cross section behaves as

$$\frac{d\sigma}{dt} \propto \frac{1}{t^2}, \quad (41)$$

which leads to a logarithmic divergence in the transport cross section at small momentum transfer.

In the present theory the gluon propagator is modified by the presence of the topological mass

$$\frac{1}{t} \rightarrow \frac{1}{t - m^2}. \quad (42)$$

The mass parameter  $m$  therefore acts as an infrared cutoff that regulates the divergence of the scattering amplitude. As a result the transport cross section becomes finite and takes the form

$$\sigma_{\text{tr}} = \frac{9g^4}{32\pi T^2} \ln\left(\frac{T^2}{m^2}\right). \quad (43)$$

It is useful to compare this behaviour with the well-known leading-order kinetic theory result for the shear viscosity of a weakly coupled gluon plasma derived by Arnold, Moore and Yaffe [8, 9]. In perturbative QCD the dominant contribution to the transport cross section also arises from  $t$ -channel gluon exchange and leads to a logarithmic enhancement associated with the infrared region of momentum transfer. In that case the infrared divergence is regulated by medium effects incorporated through the Hard Thermal Loop effective theory, which introduces a screening scale of order  $m_D \sim gT$  in the gluon propagator. In the present framework the same infrared behaviour is regulated instead by the topological gluon mass  $m$ , which therefore plays a role analogous to the screening scale in thermal QCD.

## 4 Shear viscosity of the gluonic plasma

In this section we compute the shear viscosity of the gluonic plasma using relativistic kinetic theory. Transport coefficients in a thermal plasma can be calculated using the Boltzmann equation within the framework of finite-temperature field theory [25, 26]. The viscosity is determined by the rate of momentum transport carried by quasiparticles in the medium.

## 4.1 Kinetic theory expression

For a relativistic bosonic gas the shear viscosity can be written as

$$\eta = \frac{4}{15T} \int \frac{d^3p}{(2\pi)^3} \frac{p^4}{E_p^2} \tau(p) f_0(p) [1 + f_0(p)], \quad (44)$$

where

$$E_p = \sqrt{p^2 + m^2}, \quad (45)$$

is the quasi-particle energy and

$$f_0(p) = \frac{1}{e^{E_p/T} - 1}, \quad (46)$$

is the Bose-Einstein distribution function. The shear viscosity can be computed from the Boltzmann equation describing the evolution of the gluon distribution function in the plasma. In the present work we employ the relaxation time approximation, in which the collision integral is written as

$$C[f] \approx -\frac{f - f_0}{\tau}. \quad (47)$$

This approximation captures the dominant contribution to momentum transport and is commonly used in kinetic theory estimates of transport coefficients.

## 4.2 Relaxation time

The relaxation time is related to the scattering rate of gluons in the plasma. For binary collisions the inverse relaxation time can be written as

$$\tau^{-1} = n \langle \sigma_{\text{tr}} v_{\text{rel}} \rangle, \quad (48)$$

where  $v_{\text{rel}}$  is the relative velocity of the colliding particles. For ultrarelativistic gluons in a hot plasma the relative velocity is approximately unity,  $v_{\text{rel}} \approx 1$ , so that the relaxation time reduces to

$$\tau^{-1} \approx n \sigma_{\text{tr}}. \quad (49)$$

The gluon number density is

$$n = g_g \int \frac{d^3p}{(2\pi)^3} \frac{1}{e^{p/T} - 1}, \quad (50)$$

where

$$g_g = 2(N_c^2 - 1) \quad (51)$$

is the number of gluonic degrees of freedom. The momentum integral can be evaluated using the standard Bose integral

$$\int_0^\infty \frac{x^2 dx}{e^x - 1} = 2\zeta(3). \quad (52)$$

Changing variables  $p = Tx$  gives

$$n = g_g \frac{\zeta(3)}{\pi^2} T^3. \quad (53)$$

Substituting the transport cross section derived earlier

$$\sigma_{\text{tr}} \approx \frac{9g^4}{32\pi T^2} \ln\left(\frac{T^2}{m^2}\right). \quad (54)$$

the relaxation time becomes

$$\tau \approx \frac{32\pi T^2}{9g^4 n \ln(T^2/m^2)}. \quad (55)$$

Substituting the expression for the number density yields

$$\tau \approx \frac{32\pi^3}{9g^4 g_g \zeta(3)} \frac{1}{T \ln\left(\frac{T^2}{m^2}\right)}. \quad (56)$$

### 4.3 Evaluation of the viscosity integral

We now evaluate the momentum integral appearing in the viscosity formula. For temperatures much larger than the gluon mass the energy can be approximated as

$$E_p \approx p. \quad (57)$$

The viscosity expression becomes

$$\eta = \frac{4\tau}{15T} \int \frac{d^3p}{(2\pi)^3} p^2 f_0(p) [1 + f_0(p)]. \quad (58)$$

The integral

$$I = \int \frac{d^3p}{(2\pi)^3} p^2 f_0(p) [1 + f_0(p)] \quad (59)$$

can be evaluated using the identity

$$f_0(1 + f_0) = \frac{e^{p/T}}{(e^{p/T} - 1)^2}. \quad (60)$$

Changing variables to  $x = p/T$  gives

$$I = \frac{T^5}{2\pi^2} \int_0^\infty \frac{x^4 e^x}{(e^x - 1)^2} dx. \quad (61)$$

Using the standard integral

$$\int_0^\infty \frac{x^4 e^x}{(e^x - 1)^2} dx = \frac{4\pi^4}{15}, \quad (62)$$

we obtain

$$I = \frac{2\pi^2}{15} T^5. \quad (63)$$

Substituting this result into the viscosity formula yields

$$\eta = \frac{8\pi^2}{225} \tau T^4. \quad (64)$$

#### 4.4 Final expression

Finally inserting the relaxation time gives

$$\eta \approx \frac{256\pi^5}{2025} \frac{T^3}{g^4 g_g \zeta(3) \ln(T^2/m^2)}. \quad (65)$$

The logarithmic factor  $\ln(T^2/m^2)$  originates from the integration over the small momentum transfer region of the  $t$ -channel gluon exchange. The presence of the topological mass  $m$  therefore regulates the infrared behaviour of the scattering amplitude and renders the transport cross section finite. As a result the viscosity remains finite and is controlled by the infrared scale set by the topological gluon mass.

#### 4.5 Estimate of the topological mass scale

In the previous sections the gluon mass parameter  $m$  was treated as a phenomenological parameter generated by the topological  $B \wedge F$  interaction. It is useful to estimate the expected magnitude of this mass scale in a thermal plasma.

In finite-temperature gauge theory the propagation of gauge bosons is modified by medium effects encoded in the thermal gluon self-energy [22, 25, 26]. At leading order the longitudinal component of the polarization tensor generates a screening scale known as the Debye mass. For an  $SU(N_c)$  gauge theory the Debye mass is given by

$$m_D^2 = \frac{N_c}{3} g^2 T^2, \quad (66)$$

which follows from the one-loop evaluation of the gluon polarization tensor in the thermal background [25, 26].

The origin of this scale can be understood from the hard thermal loop contribution to the gluon self-energy. Schematically one obtains

$$\Pi_{\mu\nu}(k) \sim g^2 \int \frac{d^3p}{(2\pi)^3} \frac{1}{p} f_B(p), \quad (67)$$

where  $f_B(p)$  is the Bose-Einstein distribution. Since the thermal integral is dominated by momenta of order  $p \sim T$ , dimensional analysis gives

$$\Pi_{\mu\nu}(k) \sim g^2 T^2. \quad (68)$$

This result implies that thermal gauge theories naturally generate an infrared momentum scale of order

$$m_D \sim gT. \quad (69)$$

In the present framework the gluon mass arises from the topological  $B \wedge F$  interaction rather than from thermal loop corrections. Nevertheless, the infrared behaviour of gluon exchange processes in the plasma is controlled by the same soft momentum scale. It is therefore natural to assume that the magnitude of the topological gluon mass is comparable to this scale,

$$m \sim gT. \quad (70)$$

Substituting this estimate into the expression for the viscosity obtained in the previous section gives the parametric behaviour

$$\eta \sim \frac{T^3}{g^4 \ln(1/g)}. \quad (71)$$

Consequently the ratio of shear viscosity to entropy density behaves as

$$\frac{\eta}{s} \sim \frac{1}{g^2 \ln(1/g)}. \quad (72)$$

For moderately strong coupling  $g \sim 2$  this leads to values of  $\eta/s$  of order 0.1, which is consistent with phenomenological estimates extracted from relativistic heavy-ion collision experiments.

Although this value of the coupling corresponds to a moderately strongly interacting plasma, perturbative kinetic theory calculations of QCD transport coefficients are known to remain qualitatively reliable in this regime [8, 9, 20].

## 5 Viscosity to entropy density ratio

In this section we evaluate the ratio of the shear viscosity to the entropy density of the gluonic plasma. This quantity is of particular importance in the phenomenology of the quark-gluon plasma because it controls the strength of viscous effects in relativistic hydrodynamic evolution.

### 5.1 Entropy density of the gluonic plasma

The entropy density can be obtained from the thermodynamic relation

$$s = \frac{\partial P}{\partial T}, \quad (73)$$

where  $P$  is the pressure of the system.

For a relativistic bosonic gas the pressure is

$$P = g_g \int \frac{d^3p}{(2\pi)^3} \frac{p}{3} \frac{1}{e^{p/T} - 1}. \quad (74)$$

Using the standard Bose integral

$$\int_0^\infty \frac{x^3 dx}{e^x - 1} = \frac{\pi^4}{15}, \quad (75)$$

the pressure becomes

$$P = \frac{g_g \pi^2}{90} T^4. \quad (76)$$

The entropy density is therefore

$$s = \frac{dP}{dT} = \frac{4g_g \pi^2}{90} T^3. \quad (77)$$

Thus

$$s = \frac{2g_g \pi^2}{45} T^3. \quad (78)$$

## 5.2 Ratio $\eta/s$

Using the expression for the shear viscosity derived in the previous section

$$\eta = \frac{256\pi^5}{2025} \frac{T^3}{g^4 g_g \zeta(3) \ln(T^2/m^2)}. \quad (79)$$

the ratio of shear viscosity to entropy density becomes

$$\frac{\eta}{s} = \frac{128\pi^3}{45 g_g \zeta(3)} \frac{1}{g^4 \ln(T^2/m^2)}. \quad (80)$$

## 5.3 Physical interpretation

The viscosity depends logarithmically on the topological mass parameter through the factor  $\ln(T^2/m^2)$  which acts as an infrared regulator for gluon scattering. In perturbative QCD the absence of a gluon mass leads to an infrared divergence in the transport cross section and the viscosity becomes very large. In contrast, the topological gluon mass provides a natural infrared cutoff which enhances the scattering rate of gluons in the plasma. As a result the viscosity is reduced. The gluon mass parameter appearing in the present framework originates from the topological  $B \wedge F$  interaction and is therefore present already at tree-level in the effective gauge theory. This mass should not be identified directly with the Debye screening mass generated by thermal loop corrections in QCD.

Nevertheless, in a thermal plasma the dominant infrared momentum scale governing gluon exchange processes is of order  $gT$ . It is therefore natural to assume that the magnitude of the topological gluon mass is comparable to this scale,

$$m \sim gT. \quad (81)$$

Substituting this estimate into the expression for  $\eta/s$  obtained above shows that the viscosity to entropy density ratio remains of order

$$\frac{\eta}{s} \sim \frac{1}{g^2}, \quad (82)$$

up to logarithmic corrections. For moderately strong coupling  $g \sim 2$  this leads naturally to values of  $\eta/s$  of order 0.1, consistent with phenomenological estimates of the quark–gluon plasma.

This result indicates that the presence of a topological gluon mass can naturally produce a small viscosity to entropy ratio for moderate values of the coupling constant.

$$\frac{\eta}{s} \approx 0.1. \quad (83)$$

The temperature dependence of the ratio  $\eta/s$  can be illustrated by plotting the result as a function of  $T/T_c$ , where  $T_c$  denotes the critical temperature of the deconfinement transition. The resulting behaviour is shown in Fig. 1.

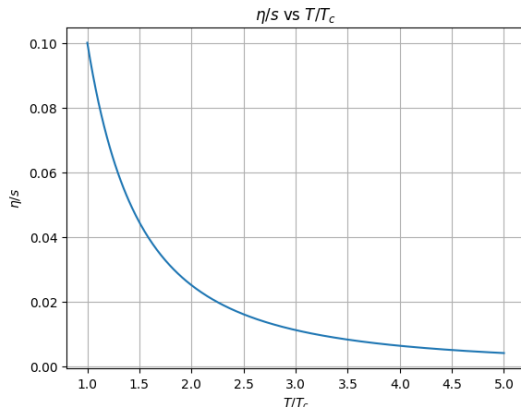


Figure 1: Ratio of shear viscosity to entropy density as a function of  $m/T$  for coupling  $g = 2$  and  $N_c = 3$ .

#### 5.4 Implications for the quark–gluon plasma

Hydrodynamic analyses of heavy–ion collision experiments indicate that the quark–gluon plasma created in relativistic nuclear collisions behaves as a nearly perfect fluid with a viscosity to entropy ratio close to

$$\frac{\eta}{s} \approx 0.1. \quad (84)$$

To illustrate the dependence of the viscosity to entropy density ratio on the topological gluon mass, it is useful to express the result in terms of the dimensionless parameter  $m/T$ . Using the expression derived above, the ratio  $\eta/s$  can be written as a function of  $m/T$ . The resulting behaviour is shown in Fig. 2.

As shown in Fig. 2, the ratio  $\eta/s$  increases with the parameter  $m/T$ . For values of the gluon mass comparable to the temperature, the resulting viscosity remains small, indicating that the plasma behaves as a nearly perfect fluid. This behaviour is consistent with the phenomenological observations of the quark–gluon plasma created in relativistic heavy–ion collisions. The

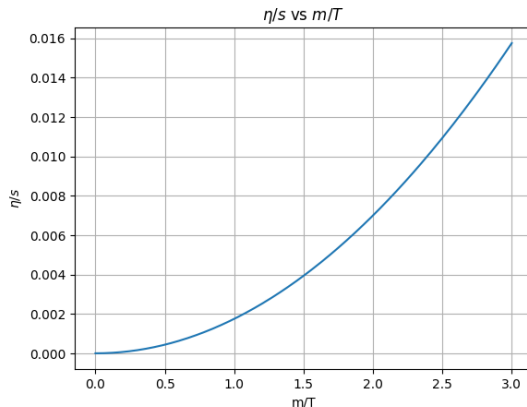


Figure 2: Temperature dependence of  $\eta/s$  as a function of  $T/T_c$  for  $g = 2$ .

plot indicates that the ratio  $\eta/s$  takes its smallest value near the transition temperature and increases as the temperature moves away from  $T_c$ . This behaviour is consistent with the picture of the quark–gluon plasma as a nearly perfect fluid near the deconfinement transition.

It is also interesting to compare the obtained values of the ratio  $\eta/s$  with the well-known Kovtun–Son–Starinets bound,

$$\frac{\eta}{s} \geq \frac{1}{4\pi}, \quad (85)$$

which was originally derived using the gauge/gravity duality. Hydrodynamic analyses of heavy-ion collision experiments suggest that the quark–gluon plasma produced in relativistic nuclear collisions has a viscosity to entropy density ratio close to this bound. The results obtained in the present framework indicate that the presence of a topological gluon mass can naturally lead to values of  $\eta/s$  in this phenomenologically relevant range.

The results obtained in the present work indicate that topological mass generation in non–Abelian gauge theories can provide a natural infrared regulator for gluon exchange processes in a hot plasma. When the topological mass scale is comparable to the soft momentum scale of the medium,  $m \sim gT$ , the resulting transport cross section leads to a shear viscosity to entropy density ratio that lies within the range extracted from hydrodynamic analyses of relativistic heavy–ion collision experiments.

The present analysis therefore suggests that topological mass generation may constitute a simple microscopic mechanism contributing to the near–

perfect fluid behaviour of the quark–gluon plasma. A more detailed understanding of this mechanism will require a systematic treatment of finite–temperature effects and the inclusion of quark degrees of freedom in the transport calculation. These questions will be explored in future work.

## 6 Conclusions

In this work we have investigated the transport properties of a gluonic plasma in a non–Abelian gauge theory where the gluons acquire a mass through a topological  $B \wedge F$  coupling. We first derived the effective massive gluon propagator obtained by integrating out the antisymmetric tensor field. The resulting propagator contains a gauge–invariant mass parameter which modifies the infrared structure of gluon exchange processes.

Using this propagator we computed the scattering amplitude for gluon–gluon interactions and derived the corresponding transport cross section. The presence of the gluon mass removes the infrared divergence which appears in perturbative QCD due to long–range gluon exchange. We then applied relativistic kinetic theory to calculate the shear viscosity of the gluonic plasma. The resulting viscosity depends on the ratio of the gluon mass scale to the temperature of the plasma and is finite due to the infrared cutoff provided by the mass term.

The ratio of shear viscosity to entropy density was also evaluated. We found that the quantity  $\eta/s$  is controlled by the dimensionless parameter  $m^2/(g^4 T^2)$ . For values of the gluon mass comparable to the temperature, the ratio  $\eta/s$  can take values close to those extracted from hydrodynamic analyses of relativistic heavy–ion collision experiments.

Our results therefore suggest that topological mass generation in non–Abelian gauge theories may provide a microscopic mechanism for the near–perfect fluid behaviour of the quark–gluon plasma. The present mechanism differs from the usual perturbative QCD treatment in that the infrared behavior of gluon exchange is regulated by a topological mass rather than by Hard Thermal Loop resummation. An important feature of the present mechanism is that the infrared behaviour of gluon exchange processes is regulated already at the level of the effective gauge theory through the topological mass term. In contrast to the conventional perturbative treatment of QCD, where infrared divergences are regulated by thermal screening effects incorporated through Hard Thermal Loop resummation, the present framework provides an intrinsic infrared cutoff in the gluon propagator. This suggests that topological mass generation may provide an alternative description of

infrared dynamics in the quark–gluon plasma. This provides a conceptually simple microscopic origin for the small viscosity of the quark–gluon plasma.

It would be interesting to explore whether the presence of a topological gluon mass could be investigated using lattice gauge theory. Lattice studies of the gluon propagator at finite temperature provide information on the infrared behaviour of gauge fields in the quark–gluon plasma. In particular, an effective mass scale for gluonic excitations can be extracted from the infrared structure of the propagator. A comparison between such lattice determinations of the finite–temperature gluon propagator and the massive propagator predicted by the present framework could provide a useful test of the role of topological mass generation in the dynamics of the quark–gluon plasma.

Several extensions of the present work are possible. In particular it would be interesting to investigate the temperature dependence of the topological gluon mass using finite–temperature field theory and to incorporate quark degrees of freedom in the transport calculation. Another important direction is the study of bulk viscosity and other transport coefficients in the same theoretical framework. These problems will be explored in future work.

## A Derivation of the transport cross section

In this appendix we derive the transport cross section relevant for momentum transport in the gluonic plasma.

### A.1 Differential cross section

For a  $2 \rightarrow 2$  scattering process the differential cross section can be written as

$$\frac{d\sigma}{dt} = \frac{|\mathcal{M}|^2}{16\pi s^2}, \quad (86)$$

where  $s$  and  $t$  are the Mandelstam variables and  $\mathcal{M}$  is the scattering amplitude.

For gluon scattering dominated by  $t$ –channel exchange, the squared matrix element takes the form

$$|\mathcal{M}|^2 = \frac{9}{2}g^4 \frac{s^2 + u^2}{(t - m^2)^2}. \quad (87)$$

In the high-energy limit where  $s \gg |t|$ , one may approximate

$$s^2 + u^2 \approx 2s^2. \quad (88)$$

The differential cross section then becomes

$$\frac{d\sigma}{dt} = \frac{9g^4}{16\pi} \frac{1}{(t - m^2)^2}. \quad (89)$$

## A.2 Definition of the transport cross section

The relevant quantity for momentum transport in the plasma is the transport cross section

$$\sigma_{\text{tr}} = \int d\sigma (1 - \cos \theta), \quad (90)$$

which suppresses forward scattering events that do not efficiently transfer momentum. Using the relation

$$\frac{d\sigma}{dt} = \frac{d\sigma}{d\Omega} \frac{d\Omega}{dt}, \quad (91)$$

the transport cross section can be written as

$$\sigma_{\text{tr}} = \int dt \frac{d\sigma}{dt} (1 - \cos \theta). \quad (92)$$

## A.3 Relation between $t$ and scattering angle

In the center-of-mass frame the Mandelstam variable  $t$  is related to the scattering angle  $\theta$  by

$$t = -2p^2(1 - \cos \theta), \quad (93)$$

where  $p$  is the magnitude of the incoming momentum. Thus

$$1 - \cos \theta = -\frac{t}{2p^2}. \quad (94)$$

Substituting this relation gives

$$\sigma_{\text{tr}} = -\frac{1}{2p^2} \int dt t \frac{d\sigma}{dt}. \quad (95)$$

## A.4 Evaluation of the integral

Substituting the differential cross section derived above yields

$$\sigma_{\text{tr}} = -\frac{9g^4}{32\pi p^2} \int dt \frac{t}{(t-m^2)^2}. \quad (96)$$

The integral

$$\int \frac{t dt}{(t-m^2)^2}, \quad (97)$$

can be evaluated explicitly, giving

$$\int \frac{t dt}{(t-m^2)^2} = \ln \left| \frac{t-m^2}{m^2} \right| + \frac{m^2}{t-m^2} + C. \quad (98)$$

where  $C$  is a constant which includes  $\ln m^2$  with integration constant. Evaluating between the approximate kinematic limits  $t_{\text{min}} \approx -s$  and  $t_{\text{max}} \approx 0$  yields

$$\sigma_{\text{tr}} = \frac{9g^4}{32\pi p^2} \ln \left( \frac{s+m^2}{m^2} \right). \quad (99)$$

Since in a thermal plasma the typical center-of-mass energy satisfies  $s \sim T^2$ , the transport cross section becomes

$$\sigma_{\text{tr}} \approx \frac{9g^4}{32\pi p^2} \ln \left( \frac{T^2}{m^2} \right). \quad (100)$$

This expression shows explicitly that the topological gluon mass provides an infrared cutoff that regulates the transport cross section.

## B Squared matrix element for gluon scattering

In this appendix we outline the steps leading from the tree-level gluon scattering amplitude to the squared matrix element used in the transport cross section.

The dominant scattering process in a gluonic plasma is

$$g(p_1) + g(p_2) \rightarrow g(p_3) + g(p_4). \quad (101)$$

The leading contribution at high temperature arises from  $t$ -channel gluon exchange.

## B.1 Tree-level amplitude

Using the Yang–Mills Feynman rules, the  $t$ -channel amplitude can be written as

$$\mathcal{M}_t = g^2 f^{abe} f^{cde} \frac{1}{t - m^2} \epsilon_1^\mu \epsilon_2^\nu \epsilon_3^\rho \epsilon_4^\sigma N_{\mu\nu\rho\sigma}, \quad (102)$$

where

$$N_{\mu\nu\rho\sigma} = \Gamma_{\mu\nu\alpha}(p_1, p_2, -k) \left( g^{\alpha\beta} - \frac{k^\alpha k^\beta}{k^2} \right) \Gamma_{\rho\sigma\beta}(-p_3, -p_4, k). \quad (103)$$

The triple-gluon vertex is

$$\Gamma_{\mu\nu\alpha}(p, q, r) = g_{\mu\nu}(p - q)_\alpha + g_{\nu\alpha}(q - r)_\mu + g_{\alpha\mu}(r - p)_\nu. \quad (104)$$

## B.2 Color averaging

To obtain the physical cross section the squared amplitude must be averaged over the colors of the incoming gluons and summed over the colors of the outgoing gluons.

For  $SU(N_c)$  one obtains

$$\sum_{a,b,c,d} f^{abe} f^{cde} f^{abf} f^{cdf} = N_c^2(N_c^2 - 1). \quad (105)$$

For  $N_c = 3$  this gives 72. After averaging over the colors of the incoming gluons a factor  $(N_c^2 - 1)^2 = 64$  appears in the denominator, giving  $72/64 = 9/8$ . Including the contributions from the dominant scattering channels leads to the effective color factor  $9/2$  used in the squared amplitude.

## B.3 Polarization sums

The squared amplitude involves a sum over the polarization states of the external gluons.

For transverse gluon polarizations the completeness relation is

$$\sum_{\lambda} \epsilon_{\mu}^{(\lambda)}(p) \epsilon_{\nu}^{(\lambda)*}(p) = -g_{\mu\nu}. \quad (106)$$

Using this relation the polarization sums can be performed and the squared matrix element takes the form

$$|\mathcal{M}|^2 = \frac{9}{2}g^4 \frac{s^2 + u^2}{(t - m^2)^2}. \quad (107)$$

This expression is valid in the high-energy limit where the dominant contribution arises from the  $t$ -channel exchange diagram.

#### B.4 Differential cross section

The differential cross section for two-body scattering is given by

$$\frac{d\sigma}{dt} = \frac{|\mathcal{M}|^2}{16\pi s^2}. \quad (108)$$

Substituting the squared amplitude gives

$$\frac{d\sigma}{dt} = \frac{9g^4}{32\pi} \frac{s^2 + u^2}{s^2(t - m^2)^2}. \quad (109)$$

In the high energy limit  $s \gg m^2$  the Mandelstam variable  $u$  satisfies

$$u \approx -s, \quad (110)$$

so that

$$s^2 + u^2 \approx 2s^2. \quad (111)$$

The differential cross section therefore reduces to

$$\frac{d\sigma}{dt} = \frac{9g^4}{16\pi} \frac{1}{(t - m^2)^2}. \quad (112)$$

## References

- [1] E. V. Shuryak, Prog. Part. Nucl. Phys. 53, 273 (2004).
- [2] M. Gyulassy and L. McLerran, Nucl. Phys. A750, 30 (2005).
- [3] U. Heinz and R. Snellings, Ann. Rev. Nucl. Part. Sci. 63, 123 (2013).
- [4] P. Romatschke and U. Romatschke, Phys. Rev. Lett. 99, 172301 (2007).
- [5] H. Song, S. A. Bass and U. Heinz, Phys. Rev. C83, 024912 (2011).
- [6] P. Kovtun, D. T. Son and A. O. Starinets, Phys. Rev. Lett. 94, 111601 (2005).

- [7] D. T. Son and A. O. Starinets, *Ann. Rev. Nucl. Part. Sci.* 57, 95 (2007).
- [8] P. Arnold, G. D. Moore and L. G. Yaffe, *JHEP* 0011, 001 (2000).
- [9] P. Arnold, G. D. Moore and L. G. Yaffe, *JHEP* 0305, 051 (2003).
- [10] S. Jeon, *Phys. Rev. D* 52, 3591 (1995).
- [11] S. Jeon and L. G. Yaffe, *Phys. Rev. D* 53, 5799 (1996).
- [12] E. Braaten and R. D. Pisarski, *Nucl. Phys. B* 337, 569 (1990).
- [13] A. Rebhan, *Phys. Rev. D* 48, R3967 (1993).
- [14] R. D. Pisarski, *Phys. Rev. Lett.* 63, 1129 (1989).
- [15] D. Z. Freedman and P. K. Townsend, *Nucl. Phys. B* 177, 282 (1981).
- [16] T. J. Allen, M. J. Bowick and A. Lahiri, *Mod. Phys. Lett. A* 6, 559 (1991).
- [17] A. Lahiri, *Phys. Rev. D* 55, 5045 (1997).
- [18] M. Henneaux and B. Knaepen, *Phys. Rev. D* 56, 6076 (1997).
- [19] G. D. Moore and O. Saremi, *JHEP* 0809, 015 (2008).
- [20] T. Schafer and D. Teaney, *Rep. Prog. Phys.* 72, 126001 (2009).
- [21] D. H. Rischke, *Prog. Part. Nucl. Phys.* 52, 197 (2004).
- [22] D. Mukhopadhyay, R. Kumar, J. E. Alam and S. K. Singh, *Phys. Rev. D* 101, 074039 (2020).
- [23] M. E. Peskin and D. V. Schroeder, *An Introduction to Quantum Field Theory*, Addison-Wesley (1995).
- [24] S. Weinberg, *The Quantum Theory of Fields Vol. II*, Cambridge University Press (1996).
- [25] J. I. Kapusta and C. Gale, *Finite-Temperature Field Theory*, Cambridge University Press (2006).
- [26] M. Laine and A. Vuorinen, *Basics of Thermal Field Theory*, Springer (2016).